INTERNATIONAL ATOMIC ENERGY AGENCY
UNITED NATIONS EDUCATIONAL, SCIENTIFIC AND CULTURAL ORGANIZATION
INTERNATIONAL CENTRE FOR THEORETICAL PHYSICS
I.C.T.P., P.O. BOX 586, 34100 TRIESTE, ITALY, CABLE: CENTRATOM TRIESTE

UNITED NATIONS INDUSTRIAL DEVELOPMENT ORGANIZATION

INTERNATIONAL CENTRE FOR SCIENCE AND HIGH TECHNOLOGY
c/o INTERNATIONAL CENTRE FOR THEORETICAL PHYSICS 34100 TRIESTE (ITALY) VIA GRIGNANO, 9 (ADRIATICO PALACE) P.O. BOX 586 TELEPHONE 040-224572 TELEFAX 040-224575 TELEX 460449 APH I

SMR/760-62

"College on Atmospheric Boundary Layer and Air Pollution Modelling"
16 May - 3 June 1994

"Lagrangian Particle Simulation of Tracer Dispersion in the Lee of a Schematic Two-Dimensional Hill"

D. ANFOSSI
Istituto di Cosmogeofisica
CNR
Turin, Italy

Please note: These notes are intended for internal distribution only.

Lagrangian Particle Simulation of Tracer Dispersion in the Lee of a Schematic Two-Dimensional Hill

G. TINARELLI,* D. ANFOSSI,% G. BRUSASCA,* E. FERRERO,* U. GIOSTRA,$,& M. G. MORSELLI,* J. MOUSSAFIR,† F. TAMPIERI,$ AND F. TROMBETTI$

*ENEL/CRAM, Servizio Ambiente, Milano, Italy; %Istituto di Cosmogeofisica, CNR, Torino, Italy; *Facolta' di Scienze, Universita' di Alessandria, Italy; $Istituto FISBAT, CNR, Bologna, Italy; &ISIATA, CNR, Lecce, Italy; †ARIA, Paris, France

(Manuscript received 20 May 1993, in final form 15 November 1993)

ABSTRACT

SPRAY, a 3D Lagrangian particle model for the simulation of complex flow dispersion, is presented. Its performance is tested against the EPA wind tunnel concentration distribution of passive tracer released from elevated point sources, located in the lee region of a two-dimensional schematic hill, in a neutrally stratified boundary layer. Based on the measured values of the first two moments of the turbulent flow velocity, the mean fields are computed over a regular grid using a mass-consistent model, whereas the turbulence structure is simply interpolated. From these fields, trajectories of tracer particles are computed using a linear formulation of the Langevin equation, with a correlated, skewed forcing. The self-consistence test (well-mixed condition), aimed at maintaining an initially well mixed particle distribution uniform in time, has shown satisfactory results in the region under study. The computed concentration field turns out to be in good agreement with the observed one. In detail, ground-level profiles and vertical cross sections of concentration are compared, showing the important effects resulting from the topographic influence on the flow structure.

1. Introduction

The growing concern for environmental problems and their management underlines the importance of correctly predicting the fate of pollutants released into the PBL and calls for new and more reliable models. This is even more essential in complex terrain where orography produces inhomogeneous fields of mean wind speed and turbulence.

Limiting the present considerations to a local scale (a few tenths of a kilometer), numerous modeling approaches can be found. We may mention the numerical Lagrangian model for reactive plumes of Stewart and Liu (1981), rotating water channel simulations performed by Alessio et al. (1992), Eulerian 3D simulations (Dawson et al. 1991), Gaussian plume models in the climatological version (Runca et al. 1982; Hanna et al. 1984; Hanna and Chang 1993), and the Lagrangian puff model (Yamada et al. 1992). In particular, Lagrangian particle models are able to yield reliable simulations of atmospheric turbulent dispersion both in flat terrain (De Baas et al. 1986; Brusasca et al. 1989, 1992; Anfossi et al. 1992) and complex terrain (McNider 1981; Segal et al. 1988; Thomson 1986). While horizontal homogeneity can be assumed in flat terrain, however, in the case of complex terrain the complete 3D structure of the turbulent flow must be considered. This means that the spatial variations of wind velocity moments should be taken into account.

Our team designed a Lagrangian particle model (SPRAY) for the simulation of dispersion in complex flows, such as the turbulent flow occurring under convective conditions or over complex terrain in real atmospheric situations and has tested its performance in situations of increasing complexity. In a previous paper (Anfossi et al. 1992) a dispersion experiment on flat terrain in the Environmental Protection Agency (EPA) wind tunnel (Khurshudyan et al. 1981, hereafter KSN) was simulated, which allowed us to test both the choice of model parameterization and the moments of the random forcing.

The purpose of the present study is to verify our dispersion model capability in well-defined and controlled situations. We therefore compare the results with the concentration data obtained in the same wind tunnel from elevated point sources in the presence of a schematic hill (KSN), using vertical and horizontal profiles of concentration measured at various downwind distances from the source. As far as flow and turbulence fields are concerned, it should be noted that in the flat terrain simulation (Anfossi et al. 1992) all the profiles measured at one place were assumed to define the whole computation domain. On the contrary, here they must be given at grid points since the presence of the hill induces both vertical and horizontal inhomogeneities.

Corresponding author address: Dr. Gianni Tinarelli, ENEL/CRTN—Via Rubattino 54, Servizio Ambiente, 20134, Milano, Italy.

The EPA wind tunnel experiments form a very useful dataset for the study of flow and dispersion over gentle orography in controlled conditions. It is worthwhile recalling that previous papers dealing with the same dataset (Arya et al. 1987; Lawson et al. 1989; Tampieri et al. 1990) were mainly devoted to an analysis of the variations in the ground-level concentration (GLC) induced by the presence of the hills with respect to the flat terrain case.

A description of the Lagrangian dispersion model is given in section 2. In section 3 the wind tunnel experiment is briefly outlined. Wind and turbulence fields and related parameterizations are presented in section 4. Section 5 deals with the results of the comparison between simulations and experiments.

2. Description of the Lagrangian dispersion model

In Lagrangian particle diffusion models turbulent dispersion is simulated by following a great number of fictitious particles released from an emission point, reconstructing the concentration field from their trajectories. In Lagrangian single-particle models, such as SPRAY, each particle trajectory represents a single statistical realization in a turbulent flow with the same macroscopic initial and boundary conditions; in this way, the motion of any two different particles is completely independent and the concentration fields must be interpreted as ensemble averages.

a. Model equations

In SPRAY each particle position is represented by a vector of three Cartesian components X_i (i = 1, 2, 3) in which the first two are horizontally directed while the third one is along the vertical. At every time step Δt, particle positions are updated using the following equations:

$$X_i(t + \Delta t) = X_i(t) + \frac{U_i(t) + U_i(t + \Delta t)}{2}\Delta t \qquad (i = 1, 2, 3) \quad (1a)$$

$$U_i(t + \Delta t) = U_i(t)\left(1 - \frac{\Delta t}{2T_{L_i}}\right)\left(1 + \frac{\Delta t}{2T_{L_i}}\right)^{-1} + \mu_i\left(1 + \frac{\Delta t}{2T_{L_i}}\right)^{-1}, \quad (1b)$$

where U_i is the ith component of the particle velocity, T_{L_i} is the Lagrangian time scale for the ith velocity component, and μ_i is the ith component of a random forcing vector, picked from a generic joint probability density function (pdf) $P(\mu_1, \mu_2, \mu_3)$. Equations (1b) are a discretized form of the linear stochastic differential Langevin equation (De Baas et al. 1986; Gardiner 1990) originally developed to describe the Brownian motion. They have been used to simulate atmospheric dispersion both in homogeneous and inhomogeneous turbulence conditions (Thomson 1984, 1986; De Baas et al. 1986; Brusasca et al. 1989). In these equations, random terms come from a generic 3D distribution not necessarily Gaussian. This allows us to take into account:

(i) the cross-correlation terms between different components of wind fluctuations;

(ii) the skewness of the wind distribution in certain directions;

(iii) the spatial variations of the turbulence fields, both vertical and horizontal (typically induced by the orography).

According to Thomson (1984), in order to prevent particle accumulations in regions with low velocity variances, a form for the pdf of the random forcing must be prescribed that depends upon the turbulence conditions in such a way that the steady-state pdf of the particles in phase space is the same as that of the air. This condition satisfies the so-called well-mixed condition, which is a form of the second law of thermodynamics (Sawford 1986) and is a necessary constraint to perform physically well based simulations (Thomson 1987). The well-mixed condition requires that an initially uniform distribution of particles is maintained after a time long enough to ensure complete decorrelation with the initial conditions.

The random forcing is theoretically assigned prescribing the complete hierarchy of the infinite moments of its pdf of the form $\mu_1^m \mu_2^n \mu_3^p$ with $m, n, p \geq 0$. In the Appendix, the formulas for the moments up to third order are reported showing the relationship with the Eulerian moments of wind components and the Lagrangian time scales. Most of these quantities can be directly measured or adequately parameterized and represent the main input parameters of SPRAY.

This scheme has been criticized by many authors (see Thomson 1987; Sawford and Guest 1987) and the related problems have been discussed in a previous work (Tampieri et al. 1992), showing that the approach is substantially acceptable and capable of giving a unique solution in a 3D domain. A different approach, based on a generalized and nonlinear form of the Langevin stochastic differential equation for the particle velocity, has been introduced by Thomson (1987), Sawford and Guest (1988), and applied by Luhar and Britter (1989) to a convective boundary layer case. This approach is theoretically more sound than the previous one but does not have a unique solution in two- or three-dimensional flows (Sawford 1993).

In our model each particle velocity component is split as follows:

$$U_i(t) = \overline{U_i(\mathbf{x}, t)} + U_i'(t), \qquad (2)$$

where $\overline{U_i(\mathbf{x}, t)}$ represents a mean value and $U_i'(t)$ is a fluctuation. Equations (1b) are then transformed into new equations describing the time evolution of the

fluctuation terms (Anfossi et al. 1992), that represent a modified form of the Langevin equations:

$$U_i'(t+\Delta t) = U_i'(t)\left(1-\frac{\Delta t}{2T_{L_i}}\right)\left(1+\frac{\Delta t}{2T_{L_i}}\right)^{-1} + \mu_i'\left(1+\frac{\Delta t}{2T_{L_i}}\right)^{-1} - U_k'\frac{\partial \overline{U_i}}{\partial x_k}\Delta t, \quad (3)$$

where

$$\mu_i' = \mu_i - \frac{\overline{U_i}}{T_{L_i}}\Delta t - \frac{\partial(\overline{U_i}U_k)}{\partial x_k}\Delta t - \left(\frac{\partial \overline{U_i}}{\partial t}\right)\Delta t \qquad i = 1, 2, 3 \quad (4)$$

are the new random components. Their moments are

$$\overline{\mu_i'} = \overline{\mu_i} - \frac{\overline{U_i}}{T_{L_i}}\Delta t - \frac{\partial(\overline{U_i}\,\overline{U_k})}{\partial x_k}\Delta t - \left(\frac{\partial \overline{U_i}}{\partial t}\right)\Delta t \quad (5)$$

$$\overline{\mu_i'\mu_j'} = \overline{\mu_i\mu_j} + O(\Delta t^2). \quad (6)$$

The velocity moments and the Lagrangian time scales should be known as a function of position x in space (lowercase letters indicate Eulerian coordinates) and time t on a three-dimensional Eulerian grid as a result of measurements or of a mathematical model. The grid is defined in a terrain-following coordinate system (x, y, s) in which the vertical coordinate s is

$$s = \frac{z_f - z_g(x, y)}{z_{\text{top}} - z_g(x, y)} \quad (7)$$

where z_f is the height above the flat ground, $z_g(x, y)$ the orography height, and z_{top} the top of domain.

To obtain the meteorological values at a particle position (X_1, X_2, X_3), the model at first translates the particle coordinates into the (x, y, s) system and then makes a linear interpolation using the values at the eight corners of the grid cell to which the particle belongs.

b. *Random forcing generation and approximations*

Thomson's (1984) complete scheme produces an infinite moment hierarchy provided that all the Eulerian turbulence moments are known. In order to preserve the correct physical information, in our implementation we assumed the joint pdf of the random forcing to be Gaussian, cross correlated with nonzero mean in the horizontal direction and asymmetric in the vertical direction. This allows us to consider both the horizontal and vertical turbulence inhomogeneities through the drift acceleration terms (Thomson 1984). This pdf takes into account all the moments up to the second order (including the cross-correlation terms) together with the skewness relative to the vertical direction, that is: $\overline{\mu_i'}$, $\overline{\mu_i'\mu_j'}$ $(i, j = 1, 2, 3)$, and $\overline{\mu_3'^3}$. The actual values for these moments can be obtained from formulas (4), and (5), and those in the Appendix. In order to build a pdf that satisfies such constraints, a generalized form of the algorithm described in Anfossi et al. (1992), which makes use of linear combinations between couples of cross-correlated Gaussian distributions, has been used.

3. Wind tunnel experiment

The tracer dispersion experiments were carried out by KSN in the EPA meteorological wind tunnel. A neutral boundary layer (NBL) over either schematic hills or flat terrain was reproduced, with the following main characteristics: height equal to 1 m, surface roughness $z_0 = 1.57 \times 10^{-4}$ m, free-stream wind speed $U_\infty = 4$ m s^{-1}, and friction velocity $u_* = 0.185$ m s^{-1}. According to the authors, this corresponds to a rural NBL about 600 m high, characterized by a z_0 of about 0.1 m. In the experiments the x axis was aligned with the mean wind direction (wind tunnel longitudinal dimension), the y axis along the crosswind direction and the z axis upward. Due to the symmetry of the experiment, the bulk flow was homogeneous in the y axis direction. Three two-dimensional hills, with the same maximum height $H = 0.117$ m but different aspect ratios (ratio of the half-length a to the maximum height) equal to 3, 5, and 8 (named H3, H5, H8) were used. The tracer, ethylene (nearly neutrally buoyant in air), was emitted from a source consisting of a porous sphere 0.015 m in diameter. Various source heights and locations (all along the tunnel centerline) were utilized during the experiments. The wind tunnel scale represents in the real world dispersion in hilly terrain up to distances of the order of 5 km.

The dataset includes: (i) flow data—the vertical profile of the mean wind speed $\overline{U_1}$ and $\overline{U_3}$, the standard deviations of wind fluctuations σ_{U_1} and σ_{U_3}, and their cross correlation $\overline{U_1'U_3'}$ (measured by hot-wire anemometer) at numerous positions upwind, over, and downwind of the model hill; (ii) concentration data—GLC values along the tunnel centerline, vertical and lateral concentration profiles at various downwind positions; the concentration C has been normalized by KSN as $\chi = CU_\infty h_r^2/Q$, where Q is the emission rate and $h_r = 0.234$ m is a reference height. The standard deviations σ_z and σ_y and centroid height $\bar{z}$ of concentration distribution as a function of the downwind distance can be computed.

We are interested in the simulation of tracer releases from point sources located in the lee of the obstacle, where the largest inhomogeneities in the flow field are observed. The less steep hill H8 has been chosen because, as pointed out by KSN, wind and turbulence measurements in the near wakes of the H3 and H5 hills could be unreliable as they were measured by hot-wire anemometers, which are unable to detect flow reversals in the separated region, if any. Nevertheless, even the gently sloping H8 produces important distortions in both the flow and concentration fields. As far

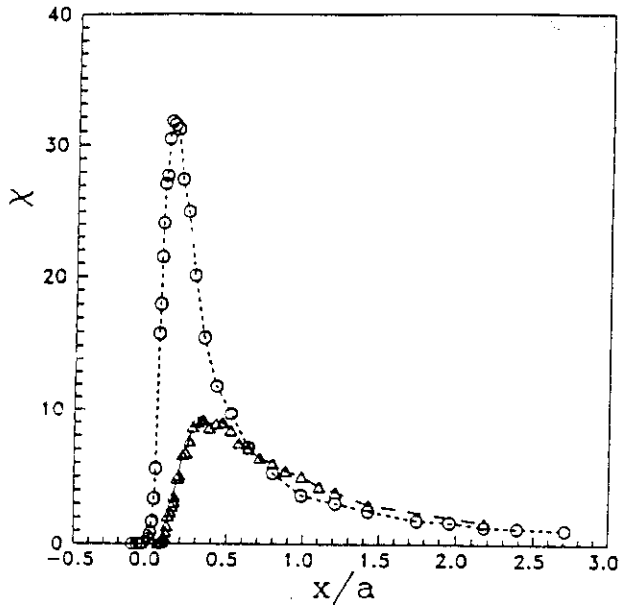

FIG. 1. Normalized GLCs as a function of downwind distance (scaled on the half hill length a), measured by KSN for a point source at height of 0.029 m: flat terrain case (triangles) and H8 case (circles) with the source located at the downwind base of the hill ($x/a = 0$).

as the GLCs are concerned, Fig. 1 is quite informative: it shows that the measured maximum GLC in the hill case is about a factor of 3 higher than in the flat terrain case and is closer to the source. Furthermore it can be seen that some tracer is found upwind of the source in the presence of the hill. This is consistent with visualization experiments conducted by KSN where, even if no average flow separation was detected, occasional puffs of smoke were observed to travel short distances up the lee slope. It should be noted that, because of the complexity of the lee region, the KSN comparison between K models and the experiment gave, in this case, the worst agreement. To investigate dispersion in different regions of the perturbed NBL, two diffusion experiments from source heights $h_s = H/4 = 0.029$ m and $h_s = H = 0.117$ m have been simulated.

4. Input data and parameterizations

The general meteorological input for the model requires the three Eulerian mean wind components $\overline{U_1}(\mathbf{x}, t)$, $\overline{U_2}(\mathbf{x}, t)$, $\overline{U_3}(\mathbf{x}, t)$, fluctuation velocity moments, and the Lagrangian time scales T_{L_1}, T_{L_2}, T_{L_3}. The symmetry characteristics of both the wind tunnel and the hill make the standard deviations of wind components σ_{U_1}, σ_{U_2}, σ_{U_3}, and the cross-correlation term $\overline{U_1' U_3'}$ the only nonzero second-order moments. All the data are reported as functions of the height above the bottom surface $z = z_f - z_g(x, y)$.

The smoothed data of mean wind vertical profiles (Trombetti et al. 1991), whose locations are shown in Fig. 2, have been used to build the initial conditions for the mass-consistent flow model MINERVE (Geai 1987), which gives a three-dimensional nondivergent mean flow field on the same terrain-following grid used by our dispersion model. The computational domain, whose horizontal and vertical dimensions are 7.4 m × 7.4 m and 2 m, respectively (see Fig. 2), is divided into 64 × 64 × 15 grid points with constant horizontal steps $\Delta x = \Delta y = 0.117$ m. This guarantees a good resolution in the description of H8, which occupies 17 grid points. The vertical steps are of variable size (smaller near the ground: the minimum being $\Delta s = 0.005$, which corresponds, over flat terrain, to $\Delta z = 0.01$ m), in order to permit a good description of large vertical gradients occurring in the region adjacent to the ground. The comparison between the experimental vertical profiles of $\overline{U_1}$ and $\overline{U_3}$ and those obtained from the MINERVE code is shown in Fig. 3 (see also Finardi et al. 1993). The root-mean-square errors between the 15 observed $\overline{U_1}$ and $\overline{U_3}$ profiles and the corresponding ones calculated by MINERVE are 0.1 and 0.04 m s^{-1}, with the maximum point-to-point errors of 0.37 and 0.09 m s^{-1}, respectively. The agreement is quite reasonable and particularly good in the region downwind of the hill, where our simulation takes place. In Figs. 4a and 4b isolines of $\overline{U_1}$ and $\overline{U_3}$ in the x–z_f plane are shown. A wake with a decrease in wind in-

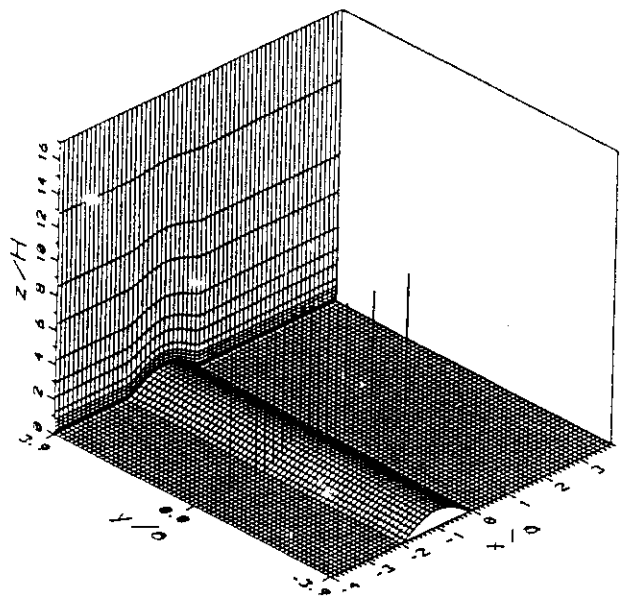

FIG. 2. Computational domain used in the simulations of dispersion from sources located at the downwind base of H8 ($x/a = 0$). Horizontal grid spacing is $\Delta x = \Delta y = 0.117$ m (i.e., $\Delta x/a = \Delta y/a = 1/8$). The vertical scale is expanded with respect to the horizontal one and the continuous lines represent the nonuniform vertical grid spacing. Vertical bars at $y = 0$ indicate the flow data measurement points.

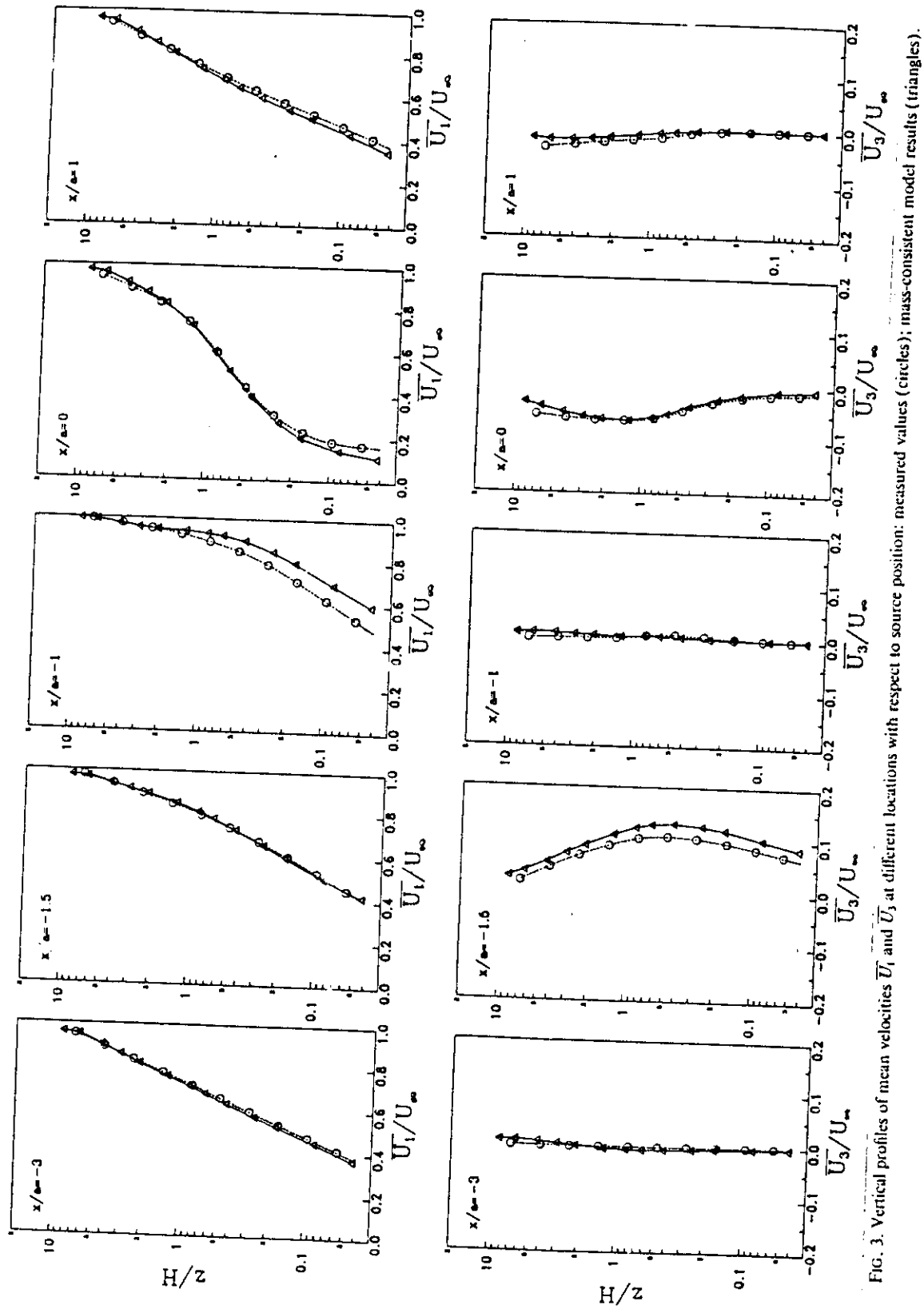

FIG. 3. Vertical profiles of mean velocities $\overline{U_1}$ and $\overline{U_3}$ at different locations with respect to source position: measured values (circles); mass-consistent model results (triangles).

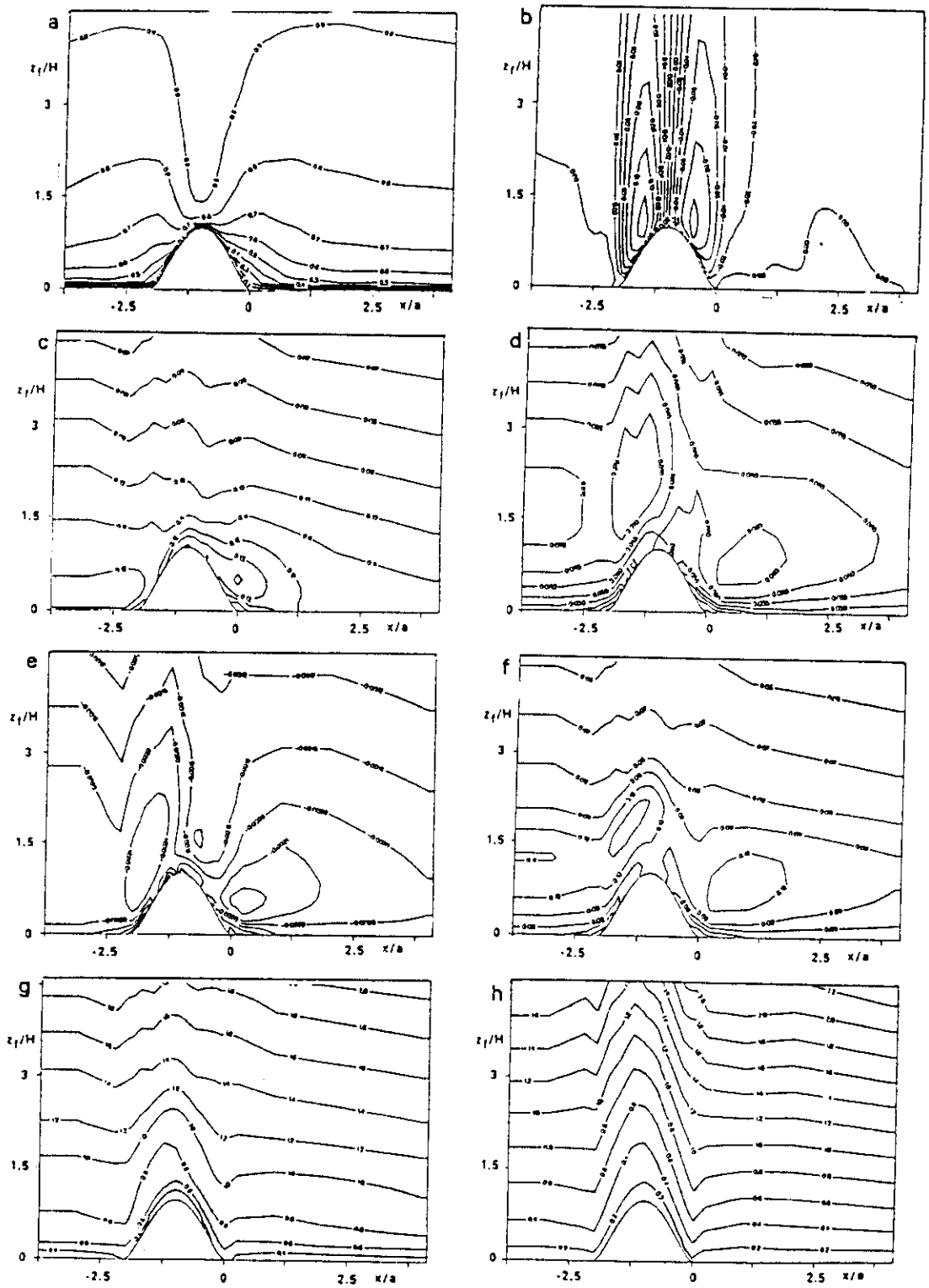

FIG. 4. Maps of model input parameters in the x-z_f plane. The vertical extent is limited in order to detail the region of major interest. (a) $\overline{U_1}/U_\infty$; (b) $\overline{U_3}/U_\infty$; (c) σ_{U_1}/U_∞; (d) σ_{U_3}/U_∞; (e) $\overline{U_1U_3}/U_\infty^2$; (f) σ_{U_2}/U_∞; (g) $T_{L_1}/T_a = T_{L_2}/T_a$, where $T_a = a/U_\infty$; (h) T_{L_3}/T_a.

tensity is present in the downwind region without flow reversal.

The smoothed vertical profiles of σ_{U_1}, σ_{U_3}, and $\overline{U_1' U_3'}$ (Trombetti et al. 1991) have been used to produce the respective 3D fields by linear interpolations at the grid points. Isolines of these fields in the x–z_f plane are shown in Figs. 4c, 4d, and 4e, which all show the existence of horizontal gradients induced by the presence of orography and highlight the lee region where the turbulence fields are stronger.

Because of its finite size, the wind tunnel is not able to simulate the effects of mesoscale horizontal eddies. As a consequence, some parameters used in the calculations are prescribed in order to match the wind tunnel conditions, not the corresponding atmospheric ones. This choice was also adopted by KSN in their simulations. Therefore, in order to simulate σ_{U_2} and horizontal Lagrangian time scales T_{L_1} and T_{L_2}, we used the parameterizations described in Trombetti and Tampieri (1992) and Anfossi et al. (1992), based on the available data and on general spectral features as described in the literature. Using vertical profiles of σ_{U_1}, σ_{U_2}, and σ_{U_3} measured over flat terrain, the following empirical relationships were found:

$$\sigma_{U_2} = \begin{cases} 1.55\sigma_{U_3}, & z \leq 0.2 \text{ m} \\ 0.85\sigma_{U_1}, & z > 0.2 \text{ m}, \end{cases}$$

and assumed to hold also in presence of the hill. Figure 4f shows the isolines of σ_{U_2} in x–z_f plane obtained using this parameterization. As far as the horizontal Lagrangian time scales are concerned, the assumption $T_{L_1} = T_{L_2}$ was adopted; T_{L_2} was estimated from the following relation:

$$T_{L_2} = \frac{\Lambda_{L_2}}{\sigma_{U_2}}$$

where Λ_{L_2} represents the Lagrangian length scale:

$$\Lambda_{L_2}^{-1} = \Lambda_0^{-1} + (cz)^{-1}.$$

To evaluate Λ_0 and c Trombetti and Tampieri (1992) showed that, because of the horizontal homogeneity, it was appropriate to apply Taylor's (1921) formula, which was used with T_{L_2} given above, to fit the lateral plume standard deviations σ_y measured for flat terrain. The values $\Lambda_0 = 0.11$ m and $c = 3.05$ were estimated. Moreover, Trombetti and Tampieri (1992) found that this parameterization worked well enough (within an error of about 25%) in the case we are dealing with. In Fig. 4g T_{L_2} isolines in the x–z_f plane are shown.

A parameterization of the Lagrangian vertical time scale, based on the vertical turbulent diffusivity K_z proposed by Berlyand and Genikhovich (1971) is used, that is,

$$T_{L_3}(x, y, z) = \frac{K_z}{\sigma_{U_3}^2} = kc_0^{1/4} \frac{\sigma_{U_1}^2(x, y, z)}{\sigma_{U_3}^2(x, y, z)} \int_0^z \frac{1}{\sigma_{U_1}(x, y, z')}\, dz',$$

where $k = 0.4$ is the von Kármán constant and $c_0 = 0.046$. In Fig. 4h isolines of T_{L_3} obtained with this parameterization are reported. In the simulations no vertical gradients of the three Lagrangian time scales are assumed near the ground, imposing the values at the ground to be equal to those at the first layer (s coordinate). The Eulerian skewness of the vertical wind fluctuations was not measured by KSN; we chose to set it equal to zero.

5. Results

In order to test the SPRAY model, two kinds of simulations were performed. The first one is a self-consistence test aimed at verifying the well-mixed condition in the presence of orography, while the second concerns the dispersion from elevated point sources.

a. Well-mixed condition

To perform the well-mixed condition test, about 50 000 particles were released uniformly into the computational domain to be advected and diffused according to the mean wind and turbulence fields previously described, for a time $t = 3T_{L_{3\max}}$, this being the maximum value for the Lagrangian time scale. This condition ensures that the final particle distribution is uncorrelated with the initial one. The time step used is $\Delta t = 0.002$ s, much smaller than the minimum value of the Lagrangian time scales. Reflecting boundary conditions were prescribed at the ground and the top of computational domain and periodic ones at the lateral boundaries.

In Fig. 5 normalized vertical concentration profiles at different points in the region considered by the diffusion experiment at $t = 0$ and $t = 3T_{L_{3\max}}$ are shown. Despite the limited number of particles used in this simulation, the average rms of the particle concentration at the different levels, computed for the plotted vertical profiles, turns out to be almost constant, giving 0.11 for the initial distribution and 0.09 for the final distribution. This shows that the model is able to maintain the well-mixed condition, satisfying the theoretical applicability requirements.

b. Simulation results

Most of the following results refer to the comparison between observed and predicted dispersion from the source at height $H/4$ (0.029 m), located at the downwind base of H8. The flow and turbulence fields used in these simulations are those previously described. Even the time step Δt is the same one utilized in the well-mixed condition test. Particles emitted from the source are advected and diffused by SPRAY up to the boundaries (reflecting boundary condition imposed at the ground). When a stationary number of particles is reached within the computational domain (about 20 000 in this simulation) the particle positions are

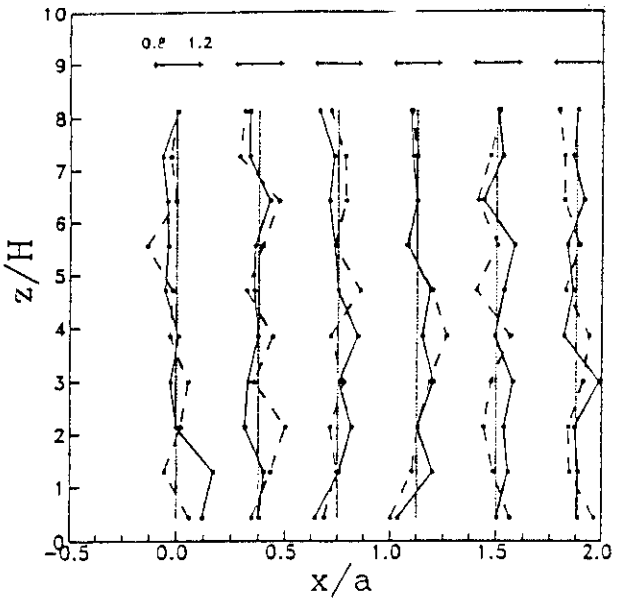

FIG. 5. Vertical profiles of the particle distribution at different distances from the H8 downwind base. $t = 0$ (dotted); $t > 3T_{L_{max}}$ (solid).

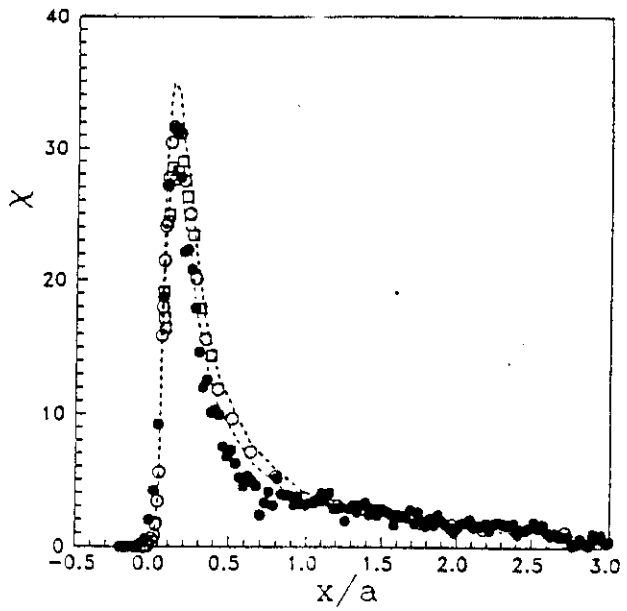

FIG. 6. Normalized GLCs as a function of downwind distance for the source at the height of 0.029 m (i.e., $H/4$): measured (circles and squares); predicted by SPRAY (dots) in each cell. Dotted lines represent the 10% experimental error band.

saved to compute concentration fields. In the present case the domain is divided into cells of volume $\Delta x \Delta y \Delta z$ ($0.025 \times 0.025 \times 0.010$ m^3) and the number of particles counted in each cell is assigned at its center. The CPU time required to move 1000 particles at each time step on a VAX station 6000/40 is about 10 s.

On some occasions two sets of concentration measurements were carried out in the EPA wind tunnel experiments and are indicated in our plots to give an idea of the scatter and uncertainty of the measured data. Moreover, KSN indicate an average relative error for each measurement of about 10%.

Measured and computed GLC values along the centerline are illustrated in Fig. 6. It appears that the overall simulation is quite satisfactory. The peak position is correctly captured and predicted results are particularly accurate near the source and in the tail of the GLC distribution. Thus, the model is capable of simulating the main expected features (see Fig. 1). Moreover, a nonnegligible amount of model particles (as well as of measured tracer) is able to travel upwind of the source. This means that, even if no average recirculation occurred, occasional flow fluctuations caused tracer motion in the direction opposite to the bulk flow.

Although most of the up-to-date dispersion models results are discussed using only GLC values, it is obvious that the spatial distribution of the concentration should be carefully computed (also for many practical applications, for instance when deposition or scavenging is evaluated), as noted by Hunt et al. (1990). Lateral and vertical concentration profiles computed at various downwind distances are shown in Fig. 7. Concerning the lateral concentration profiles, we note that all the measurements were performed at ground level with the exception of those at $x/a = 0.08$, which were carried out at 0.03 m (about the source height). The scatter appearing in many plots is due to the limited

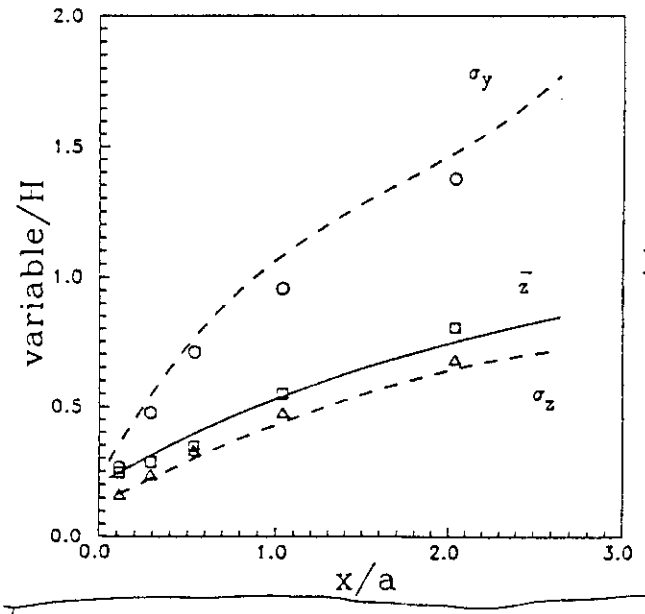

FIG. 7. Lateral (left column) and vertical (right column) profiles of normalized concentration at different downwind positions: measured (circles and squares); computed by SPRAY (dots) in each cell. Dotted lines represent the 10% experimental error band.

Fig. 8

at page 9

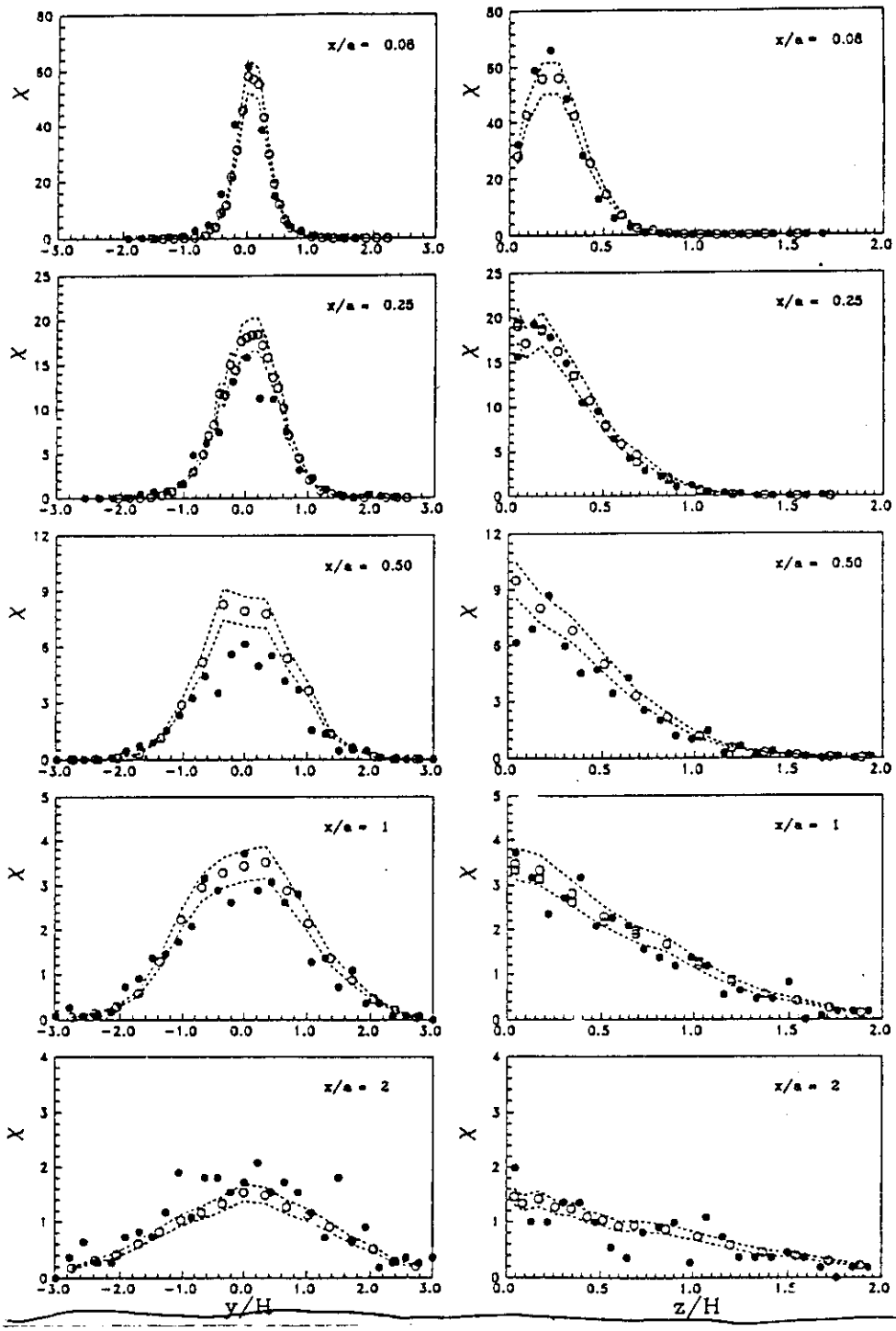

Fig. 7

FIG. 8. Lateral (σ_y: circles) and vertical (σ_z: triangles) standard deviations and centroid height ($\bar{z}$: squares) of the concentration distribution as a function of downwind distance. Symbols refer to values obtained from measured concentration profiles and lines are the best fits of the values computed from SPRAY profiles.

Let page 8

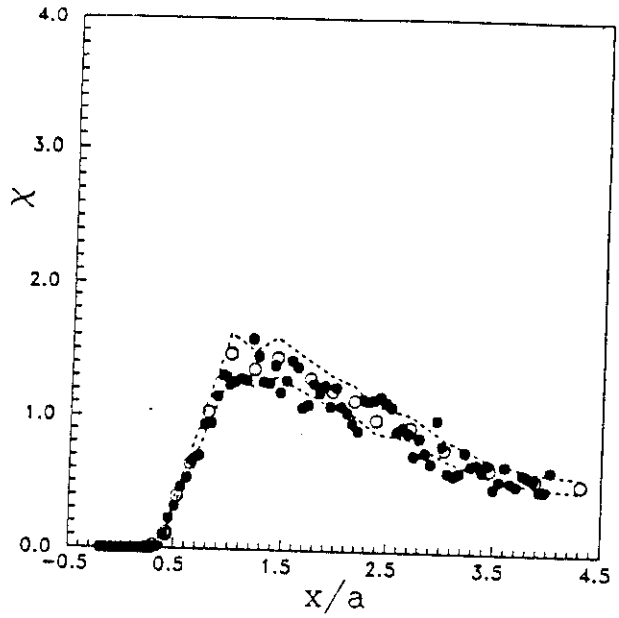

FIG. 9. As in Fig. 6, but with the source at the height of 0.117 m (i.e., H).

number of particles used in the simulations. As a general rule, the larger the number of particles, the smoother the resulting concentration profiles, since the associated error decreases as the square root of the particle number. However, our experience suggests that any further increase over an empirically determined threshold does not improve the accuracy of the results but only slightly reduces the scatter. To obtain a more quantitative evaluation of our model's performance, we computed some statistical indexes, taking into account all pairs of 3D observed–predicted concentrations (282 data). The following statistics were obtained: normalized mean-square error 0.208, correlation coefficient 0.970, and fractional bias 0.014. The agreement between predicted and measured concentrations is noticeable, giving further evidence to the good and reliable performance of our model.

From vertical and horizontal concentration profiles evaluated at different downwind distances from the source, $\bar{z}$, σ_z, and σ_y were computed as the centroid and the standard deviations of the particle distribution. Figure 8 shows that the simulation reproduces quite well the measured values that were obtained as averages weighted with the concentration data (at variance with KSN, who interpolated the profiles with analytical curves). With reference to the σ_y trend, this result means that the parameterization of crosswind turbulence is satisfactory.

Finally, Fig. 9 depicts the comparison between observed and predicted GLC distribution of tracer emitted from the source 0.117 m high (equal to the hill height). The horizontal cell dimensions (Δx, Δy) were doubled with respect to the previous case to account for the smaller number of particles near the ground. This simulation was carried out in order to assess the ability of our model (considered in its main components: the reconstruction of flow and turbulence and the diffusion determination) to simulate dispersion in a different part of the NBL where the influence of the upwind hill is quite different, as can be clearly seen from the comparison between Fig. 6 and Fig. 9. Nevertheless, the GLC (Fig. 9) and the vertical and lateral concentration profiles (not shown here) also turn out to be satisfactory for the higher source. In fact, taking into account the 195 pairs of observed–predicted concentrations, the following statistics were obtained: normalized mean-square error 0.030, correlation coefficient 0.988, and fractional bias 0.015.

KSN computed the terrain correction factor (TCF) (which gives an idea of the increased maximum GLC of the hilly simulation compared to the flat terrain case) by means of their K model. Table 1 shows that their results compared to the measured ones and to the SPRAY predictions. As can be seen, SPRAY performs quite well.

6. Conclusions

A 3D Lagrangian particle model (SPRAY) developed to deal with dispersion over complex terrain was tested against tracer diffusion data collected in the KSN wind tunnel experiment. Using this model, the concentration field of the tracer emitted at the downwind base of a two-dimensional hill was simulated. The comparison between predicted and measured results, discussed in section 5, appears to be quite satisfactory. This is due, on the one hand, to the comprehensive and accurate experimental dataset considered, which allowed us to reconstruct quite well the flow and turbulence field, and on the other, to the appropriate choice of each model component. Good results also emerge from the consistence test (well-mixed condition) which indicates that SPRAY is able to keep well mixed for a period greater than three times $T_{L_{3max}}$ an NBL initially well mixed in the lee region.

In relation to the above results the following points should be borne in mind:

(i) Thomson's (1984) model, though presenting some theoretical problems (Thomson 1987; Sawford and Guest 1988), is to our knowledge the simplest full 3D particle model available. On the other hand, Tampieri et al. (1992) showed that, providing some care is taken in the choice of the random velocities generated

TABLE 1. Terrain correction factors for maximum GLC.

h_s (m)	Observed	KSN	SPRAY
0.029	3.43	1.42	3.63
0.117	2.39	1.[illegible]	2.18

by the above-discussed random forcing, the well-mixed condition may be adequately satisfied. Thomson's new proposal (1987) while solving some problems, also poses a further difficulty, as Sawford and Guest (1988) and Sawford (1993) have shown: that is, it does not assure a unique solution in 3D flows.

(ii) The comparison between observed and predicted vertical and horizontal concentration profiles highlights the accuracy of the model in reproducing the complete 3D concentration field.

(iii) The results obtained in the present paper show that our model is quite flexible, as it is able to work in different parts of the H8 lee region. The model also gave good results for flat terrain (Anfossi et al. 1992).

(iv) The goodness of the simulation results implies that the reconstruction of the mean wind field in the lee region, obtained by our mass consistent model is satisfactory. The same holds true for the interpolation scheme and the parameterization adopted for the turbulent fields.

A comment concerning the application of SPRAY to the real atmosphere may be appropriate. At first, special attention should be paid to the definition of mean flow and turbulence fields. In fact, apart from the technical quality incorporated into a model, its performance depends on the quality of the meteorological input. We plan to derive this input mostly from measurements obtained by Doppler sodar, sonic anemometers, and standard meteorological stations properly integrated by suitable models (from mass-consistent to second-order closure models). The turbulent values not available from direct measurements or model outputs, like the Lagrangian time scales, will be assigned according to some parameterization schemes, such as those proposed by Hanna (1982) and Hanna and Chang (1993).

Moreover, the understanding of the processes of turbulent dispersion in the atmospheric boundary layer and the increased accuracy in the observations has evidenced that approaches based on the Gaussian-type formulations or even on K theory show substantial differences between the model results and the experimental data (Brown et al. 1993). On the contrary, particle models showed better agreement over flat terrain both in windy and in low wind conditions (Brusasca et al. 1989 and 1992). In complex terrain, regions of very small mean velocity exist in conjunction with very high turbulence intensity. This requires the inclusion in the model of the longitudinal diffusion, which is not accounted for by simple models but is considered by SPRAY.

In conclusion, SPRAY seems to take into explicit account some peculiarities of the dispersion in complex flow and, as such, could constitute a useful tool in conducting accurate simulations in the real atmosphere.

Acknowledgments. The authors are grateful to Dr. W. H. Snyder for supplying the dataset utilized in this study. Some authors (Anfossi, Ferrero, Giostra, Tampieri, and Trombetti) were partially supported by the CNR-ENEL project "Interactions of Energy Systems with Human Health and Environment," Rome, Italy.

APPENDIX

Moments of the Random Forcing Probability Density Function

The first three moments of the random forcing pdf in accordance with Thomson (1984) and Tampieri et al. (1992) are:

$$\overline{\mu_i} = \frac{\partial}{\partial x_k}(\overline{U_i U_k})\Delta t - \frac{\partial}{\partial x_k}(\overline{U_i U_k}) + O(\Delta t^2) = \frac{\partial}{\partial x_k}(\overline{U_i' U_k'})\Delta t + O(\Delta t^2)$$

$$\overline{\mu_i \mu_j} = \Delta t\left(\frac{1}{T_{L_i}} + \frac{1}{T_{L_j}}\right)(\overline{U_i U_j} - \overline{U_i}\,\overline{U_j}) + \Delta t\left(\frac{\partial}{\partial x_k}\overline{U_i U_j U_k} - \overline{U_i}\frac{\partial}{\partial x_k}\overline{U_j U_k} - \overline{U_j}\frac{\partial}{\partial x_k}\overline{U_i U_k}\right) + O(\Delta t^2)$$

$$= \Delta t\left(\frac{1}{T_{L_i}} + \frac{1}{T_{L_j}}\right)\overline{U_i' U_j'} + \Delta t\left(\overline{U_i' U_k'}\frac{\partial}{\partial x_k}\overline{U_j} + \overline{U_j' U_k'}\frac{\partial}{\partial x_k}\overline{U_i} + \overline{U_k}\frac{\partial}{\partial x_k}\overline{U_i' U_j'} + \frac{\partial}{\partial x_k}\overline{U_i' U_j' U_k'}\right) + O(\Delta t^2)$$

$$\overline{\mu_i \mu_j \mu_k} = \frac{\Delta t}{T_{L_i}}(\overline{U_j U_k U_i} + 2\overline{U_i}\,\overline{U_j}\,\overline{U_k} - \overline{U_j}\,\overline{U_k U_i} - \overline{U_k}\,\overline{U_j U_i} - \overline{U_i}\,\overline{U_j U_k})$$

$$+ \frac{\Delta t}{T_{L_i}}(\overline{U_i U_k U_j} + 2\overline{U_i}\,\overline{U_k}\,\overline{U_j} - \overline{U_i}\,\overline{U_k U_j} - \overline{U_k}\,\overline{U_i U_j} - \overline{U_j}\,\overline{U_i U_k})$$

$$+ \frac{\Delta t}{T_{L_k}}(\overline{U_i U_j U_k} + 2\overline{U_i}\,\overline{U_j}\,\overline{U_k} - \overline{U_i}\,\overline{U_j U_k} - \overline{U_j}\,\overline{U_i U_k} - \overline{U_k}\,\overline{U_i U_j})$$

$$+ \Delta t\left(\frac{\partial}{\partial x_l}\overline{U_iU_jU_kU_l}\right) - \Delta t\left\{\overline{U_iU_j}\frac{\partial}{\partial x_l}\overline{U_kU_l} + \overline{U_iU_k}\frac{\partial}{\partial x_l}\overline{U_jU_l} + \overline{U_jU_k}\frac{\partial}{\partial x_l}\overline{U_iU_l}\right\}$$

$$+ -\Delta t\left\{\overline{U_iU_j}\frac{\partial}{\partial x_l}\overline{U_kU_l} + \overline{U_iU_k}\frac{\partial}{\partial x_l}\overline{U_jU_l} + \overline{U_jU_k}\frac{\partial}{\partial x_l}\overline{U_iU_l}\right\}$$

$$+ 2\Delta t\left\{\overline{U_i}\,\overline{U_j}\frac{\partial}{\partial x_l}\overline{U_kU_l} + \overline{U_i}\,\overline{U_k}\frac{\partial}{\partial x_l}\overline{U_jU_l} + \overline{U_j}\,\overline{U_k}\frac{\partial}{\partial x_l}\overline{U_iU_l}\right\} + O(\Delta t^2),$$

where $i, j, k, l = 1, 2, 3$, the velocity splitting $U_i = \overline{U_i} + U_i'$ holds, and nondivergence of mean wind $(\partial/\partial x_i)\overline{U_i} = 0$ has been imposed.

In the SPRAY model, only the third pure vertical moment ($i = j = k = 3$) is retained in the following simplified form:

$$\overline{\mu_3^3} = 3\Delta t\left[\frac{\overline{U_3'^3}}{T_{L_i}} - \overline{U_3'^2}\left(\frac{\partial}{\partial x_1}\overline{U_1'U_3'} + \frac{\partial}{\partial x_2}\overline{U_2'U_3'} + \frac{\partial}{\partial x_3}\overline{U_3'^2}\right) + 2\overline{U_3'^2}\frac{\partial}{\partial x_3}\overline{U_3'^2}\right].$$

REFERENCES

Alessio, S., L. Briatore, G. Elisei, E. Ferrero, C. Giraud, A. Longhetto, and O. Morra, 1992: Laboratory simulation of Coriolis effects on atmospheric dispersion of airborne tracers over a complex terrain. *Nuovo Cimento*, **15C**, 461–472.

Anfossi, D., E. Ferrero, G. Brusasca, G. Tinarelli, U. Giostra, F. Tampieri, and F. Trombetti, 1992: Dispersion simulation of a wind tunnel experiment with Lagrangian particle models. *Nuovo Cimento*, **15C**, 139–158.

Arya, S. P. S., M. E. Capuano, and L. C. Fagen, 1987: Some fluid modeling studies of flow and dispersion over two-dimensional hills. *Atmos. Environ.*, **21**, 753–764.

Berlyand, M. E., and E. L. Genikhovich, 1971: Atmospheric diffusion and the structure of the air flow above an inhomogeneous surface. *Proc. Int. Symp. on Meteor. Aspects Air Pollution, 1968, Leningrad*, Hydrometeor Press, 49–69.

Brown, M. J., S. P. Arya, and W. H. Snyder, 1993: Vertical dispersion from surface and elevated releases: An investigation of a non-Gaussian plume model. *J. Appl. Meteor.*, **32**, 490–505.

Brusasca, G., G. Tinarelli, and D. Anfossi, 1989: Comparison between the results of a Monte Carlo atmospheric diffusion model and tracer experiment. *Atmos. Environ.*, **23**, 1263–1280.

——, ——, and ——, 1992: Particle model simulation of diffusion in low windspeed stable conditions. *Atmos. Environ.*, **26A**, 707–723.

Dawson, P., D. E. Stock, and B. Lamb, 1991: The numerical simulation of airflow and dispersion in three-dimensional atmospheric recirculation zones. *J. Appl. Meteor.*, **30**, 1005–1024.

De Baas, H. F., H. Van Dop, and F. T. M. Nieuwstadt, 1986: An application of the Langevin equation for inhomogeneous conditions to dispersion in a convective boundary layer. *Quart. J. Roy. Meteor. Soc.*, **112**, 165–180.

Finardi, S., G. Brusasca, M. G. Morselli, F. Trombetti, and F. Tampieri, 1993: Boundary-layer flow over analytical two-dimensional hills: A systematic comparison of different models with wind tunnel data. *Bound.-Layer Meteor.*, **63**, 259–291.

Gardiner, C. W., 1990: *Handbook of Stochastic Methods*. Springer-Verlag, 442 pp.

Geai, P., 1987: Methode d'interpolation and reconstitution tridimensionelle d'un champ de vent: le code d'analyse objective MINERVE. E.d.F. Chatou (France), Report DER/HE/34-87.03.

Hanna, S. R., 1982: Applications in air pollution modeling. *Atmospheric Turbulence and Air Pollution Modelling*, F. T. M. Nieuwstadt and H. Van Dop, Eds., D. Reidel, 275–310.

——, and J. C. Chang, 1993: Hybrid Plume Dispersion Model (HPDM) improvements and testing at three field sites. *Atmos. Environ.*, **27A**, 1491–1508.

——, B. A. Egan, C. J. Vaudo, and A. J. Curreri, 1984: A complex terrain dispersion model for regulatory applications at the Vestvaco Luke Mill. *Atmos. Environ.*, **18**, 685–699.

Hunt, J. R. C., R. J. Holroyd, D. J. Carruthers, A. G. Robins, D. D. Apsley, F. B. Smith, and D. J. Thomson, 1990: Developments in modelling air pollution for regulatory uses. *Proc. of 18th Int. Tech. Meeting on Air Pollution Modelling and Its Application*, Vancouver, Canada, NATO/CCMS, 1–48.

Khurshudyan, L. H., W. H. Snyder, and I. Y. Nekrasov, 1981: Flow and dispersion of pollutants over two-dimensional hills: Summary report on Joint Soviet–American Study. Rep. No. EPA-600/4-81-067, Env. Prot. Agency, 131 pp.

Lawson, R. E. Jr., W. H. Snyder, and R. S. Thompson, 1989: Estimation of maximum surface concentrations from sources near complex terrain in neutral flow. *Atmos. Environ.*, **23**, 321–331.

Luhar, A. K., and R. E. Britter 1989: A random walk model for dispersion in inhomogeneous turbulence in a convective boundary layer. *Atmos. Environ.*, **23**, 1191–1924.

McNider, R. T., 1981: Investigation of the impact of topographic circulations on the transport and dispersion of air pollutants. Ph.D. dissertation, University of Virginia.

Runca, E., A. Longhetto, and G. Bonino, 1982: Validation and physical parameterization of a Gaussian climatological model applied to a complex site. *Atmos. Environ.*, **16**, 259–266.

Sawford, B. L., 1986: Generalized random forcing in random-walk turbulent dispersion models. *Phys. Fluids*, **29**, 3582–3585.

——, 1993: Recent developments in the Lagrangian stochastic theory of turbulent dispersion. *Bound.-Layer Meteor.*, **62**, 197–215.

Sawford, B. L., and F. M. Guest, 1987: Lagrangian stochastical analysis of flux gradient relationships in the convective boundary layer. *J. Atmos. Sci.*, **44**, 1152–1165.

——, and ——, 1988: Uniqueness and universality of Lagrangian stochastic models of turbulent dispersion. *Proc. of 8th Symposium on Turbulence and Diffusion*, San Diego, CA, Amer. Meteor. Soc., 96–99.

Segal, M., R. A. Pielke, R. W. Arritt, M. D. Moran, C. H. Yu, and D. Henderson, 1988: Application of a mesoscale atmospheric dispersion modeling system to the estimation of SO2 concentrations from major elevated sources in Southern Florida. *Atmos. Environ.*, **22**, 1319–1334.

Stewart, D. A., and M. K. Liu, 1981: Development and application of a reactive plume model. *Atmos. Environ.*, **15**, 2377–2393.

Tampieri, F., F. Trombetti, and U. Giostra, 1990: A case study of dispersion in the lee of an obstacle. *Nuovo Cimento*, **13C**, 1007–1016.

——, C. Scarani, U. Giostra, G. Brusasca, G. Tinarelli, D. Anfossi, and E. Ferrero, 1992: On the application of random flight dispersion models in inhomogeneous turbulent flows. *Ann. Geophys.*, **10**, 749–758.

Taylor, G. I., 1921: Diffusion by continuous movements. *Proc. London Math. Soc. (2)*, **20**, 196–202.

Thomson, D. J., 1984: Random walk modelling of diffusion in inhomogeneous turbulence. *Quart. J. Roy. Meteor. Soc.*, **110**, 1107–1120.

——, 1986: A random-walk model for dispersion in turbulent flows and its application to dispersion in a valley. *Quart. J. Roy. Meteor. Soc.*, **112**, 511–530.

——, 1987: Criteria for the selection of stochastic models of particle trajectories in turbulent flows. *J. Fluid Mech.*, **180**, 529–556.

Trombetti, F., and F. Tampieri, 1992: Analysis of wind tunnel dispersion data over two-dimensional obstacles. *Bound.-Layer Meteor.*, **59**, 209–226.

——, P. Martano, and F. Tampieri, 1991: Data set for studies of flow and dispersion in complex terrain: i) the "RUSHIL" wind tunnel experiment (flow data). Technical Report N. 1, FISBAT-RT-91/1, 132 pp.

Yamada, T., S. Bunker, and M. Moss, 1992: Numerical simulation of atmospheric transport and diffusion over coastal complex terrain. *J. Appl. Meteor.*, **31**, 565–578.

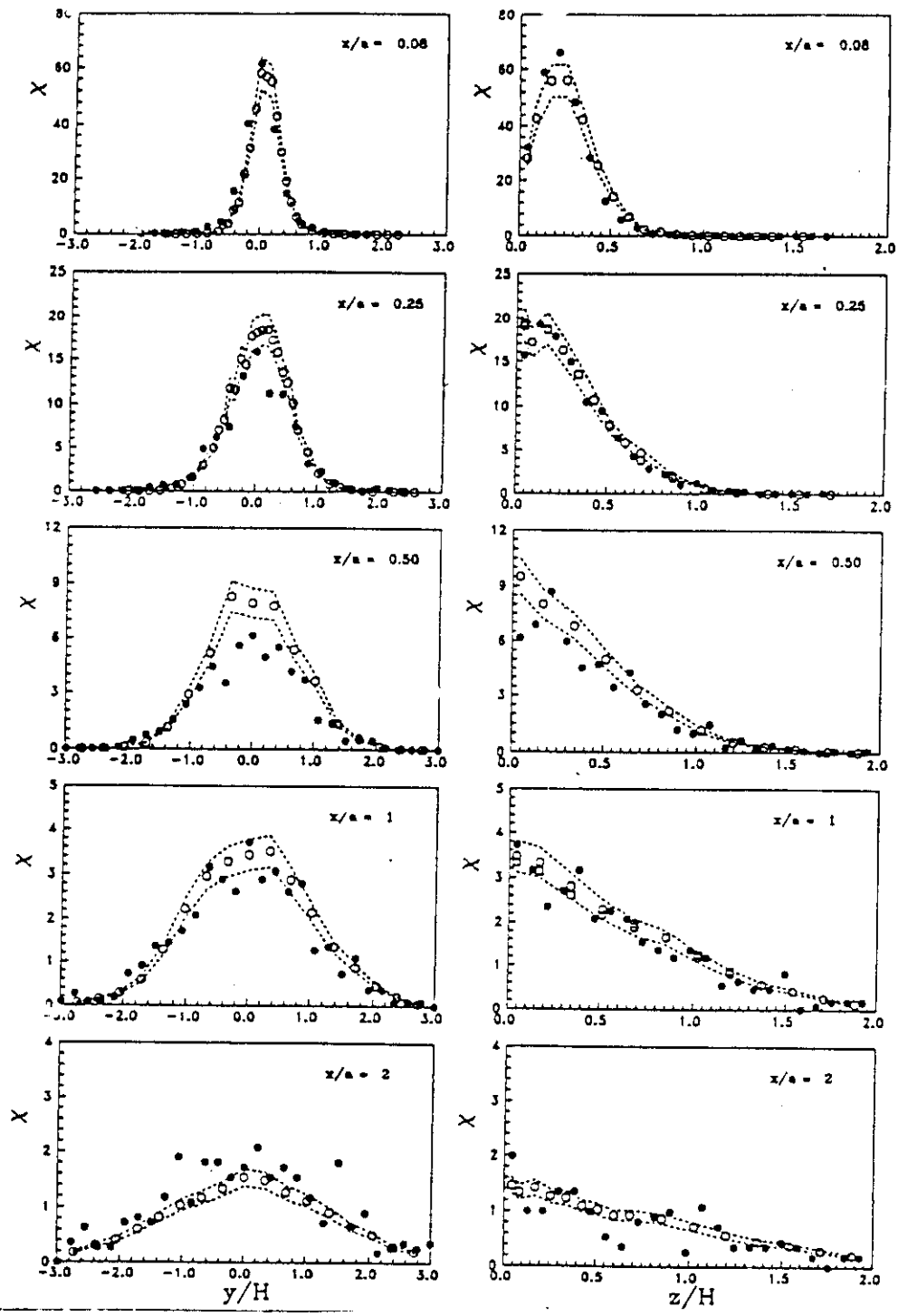

FIG. 7. Lateral (left column) and vertical (right column) profiles of normalized concentration at different downwind positions: measured (circles and squares); computed by SPRAY (dots) in each cell. Dotted lines represent the 10% experimental error band.

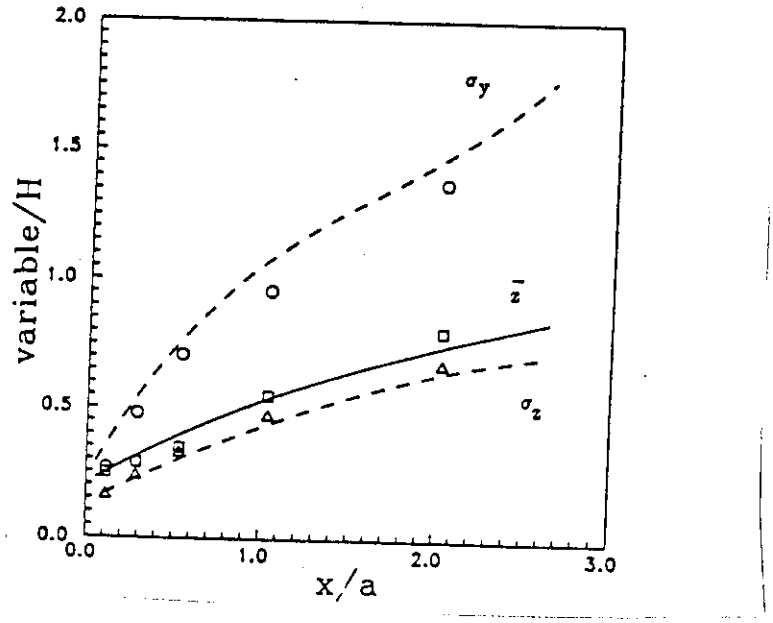

FIG. 8. Lateral (σ_y: circles) and vertical (σ_z: triangles) standard deviations and centroid height ($\bar{z}$: squares) of the concentration distribution as a function of downwind distance. Symbols refer to values obtained from measured concentration profiles and lines are the best fits of the values computed from SPRAY profiles.